

Ultimate Strength Prying Models for Bolted T-stub Connections

JAMES A. SWANSON

ABSTRACT

Several recognized prying models are discussed and evaluated using experimental data collected during 21 component tests conducted as part of a SAC investigation at the Georgia Institute of Technology as a basis. Four existing prying models are considered in addition to the model that appears in the European design specification. A modification of an existing design model is proposed.

INTRODUCTION

In the recent past, several research projects have been conducted to investigate bolted connection behavior. One of those projects, SAC subtask 7.03, was conducted at the Georgia Institute of Technology and focused on bolted T-stub connections (Figure 1) as an alternative to fully welded connections for light to moderate beam sizes. Several behavioral characteristics of T-stub connections were examined including strength, stiffness, and deformation capacity. The experimental program was broken into two phases. During the first phase, the component testing phase, 48

individual T-stubs were subjected to axial loads. During the second phase, the connection testing phase, complete T-stub connection assemblies were subjected to moments. The goal of testing individual T-stubs as components was to allow a larger number of parameters to be systematically varied than would have been feasible using connection tests. A discussion of the experimental program was provided by Swanson and Leon (2000) and additional modeling issues are addressed in Swanson and Leon (2001) and Swanson, Kokan, and Leon (2001). The focus of this paper will be the strength of T-stubs that fail with the formation of a prying mechanism in their flange.

The determination of the ultimate strength of a T-stub component subjected to an axial load is a complex process. Of the possible failure modes, the most studied case is the development of a bending mechanism in the T-stub flange followed by failure of the tension bolts (i.e. the formation of a prying mechanism). In this paper, existing prying models will be evaluated by comparing their predictions to the results of 21 of the Georgia Tech component tests that failed as a result of tension bolt fractures. Several models for predicting the ultimate strength of T-stub connections are available. Most are based on work by Struik and de Back (1969), Nair, Birkemoe, and Munse (1974), Douty and McGuire (1965), or Jaspart and Maquoi (1991). Because the model proposed by Struik and de Back provided very good results, it will be discussed in the most detail.

BACKGROUND

In this discussion of the existing models, the notations used by the various authors will be converted to that used in this work so that a clearer comparison can be made. The notation that will be used is illustrated in Figures 2 and 3. The analysis of a T-stub flange is made easier by considering a width of the T-stub that is tributary to one pair of bolts. This tributary width will be called p and can be calculated as

$$p = \frac{2 \times W_{T-stub}}{n_{tb}} \quad (1)$$

where

W_{T-stub} = the width of the T-stub at the column flange
 n_{tb} = the number of tension bolts connecting the T-stub flange

Other parameters that appear in the discussion of T-stubs are:

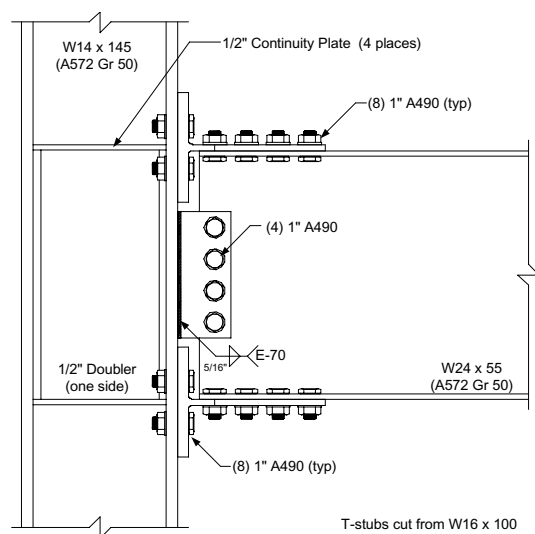


Fig. 1. Typical bolted T-stub moment connection.

James A. Swanson is assistant professor, department of civil and environmental engineering, University of Cincinnati, Cincinnati, OH.

- T = the applied T-stub tension per tension bolt
 B = the force present in a tension bolt at any given time
 B_n = the tensile capacity of a bolt
 B_o = the initial pretension of a bolt
 Q = the prying force per bolt
 g_i = the distance between the center lines of the tension bolts
 a = the distance measured from the bolt line to the edge of the T-stub flange
 b = the distance from the bolt line to the face of the T-stem

Other parameters that are specific to particular models will be introduced as needed. It is crucial to understand that T is the applied T-stub load per tension bolt and is the load that is applied to one half of the tributary width of a T-stub. Therefore, the total applied load is equal to $T \times n_{lb}$.

In all of the models considered in this work, a prying force is assumed to develop as the flange deforms. This prying force is added to the conventional force present in the tension bolts lowering the applied load that can be safely applied to the T-stub. The basic mechanism is shown in Figure 2 and fundamental equilibrium shows that the bolt tension is the sum of the prying force and applied load, $B = T + Q$. The prying forces can generally be minimized by reducing the tension bolt gage or by increasing the flange thickness. The assumption that the prying forces act at the

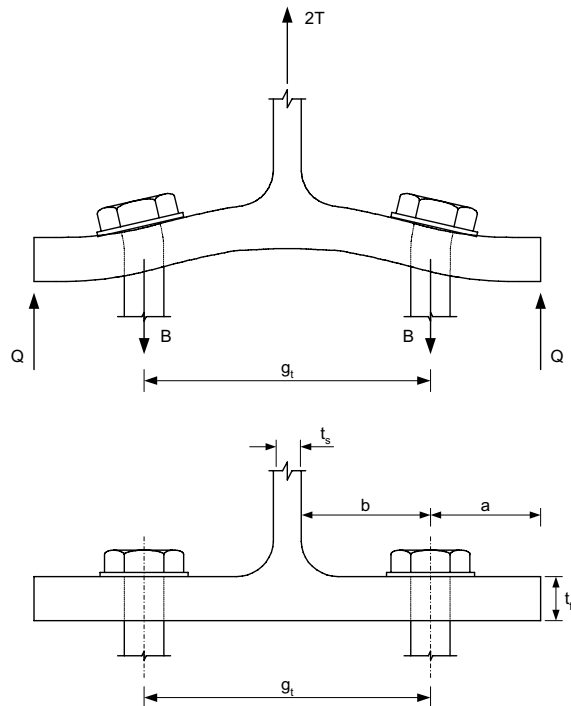


Fig. 2. Typical flange prying mechanism.

tips of the flange is generally accepted and is considered accurate until the length of the flange exterior to the bolt becomes large or until the flange thickness becomes small. Figure 4 shows the flange of a T-stub prior to a tension bolt fracture.

STRUIK AND DE BACK MODEL

The prying model developed by Struik and de Back (Struik and de Back, 1969; Kulak, Fisher, and Struik, 1987) for ultimate strength prediction is the one most widely used. Variations of the model are used by the LRFD Specification (AISC, 1993), the Canadian steel design code (CISC, 1997) and the EUROCODE 3 (Eurocode, 1993). Figure 3 shows

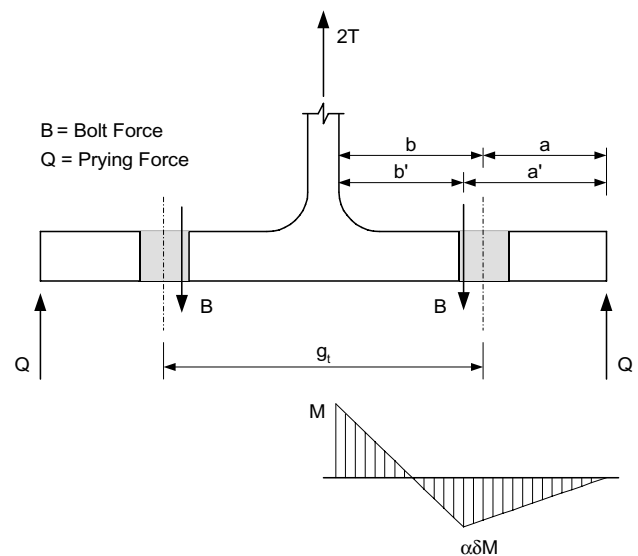


Fig. 3. Prying model of Struik and de Back (1969).

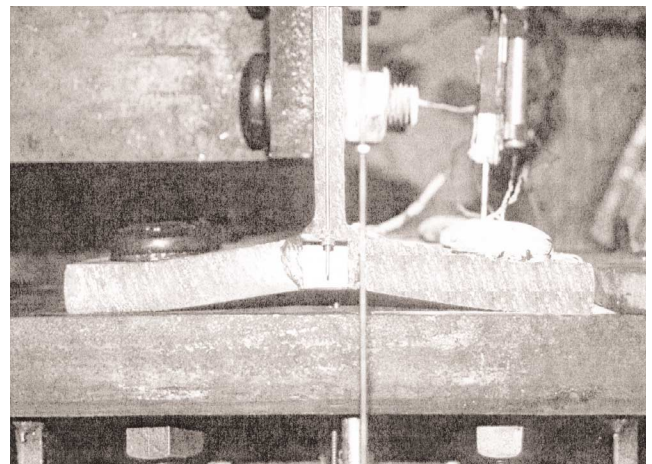


Fig. 4. T-stub flange prying prior to tension bolt fracture.

the notation and dimensions used. In this model, the bolt force is assumed to act at the inside edge of the bolt shank as opposed to acting at the centerline of the bolt. This assumption is based on the assumed load transfer from the bolt head to the flange that is shown in Figure 5. This pressure distribution is the product of the stiffness of the bolt head and the degree of bending present in the flange and bolt. As a result, equilibrium is based on the dimensions a' and b' instead of a and b . Equations 2 and 3 show the definitions of a' and b' .

The prying forces, Q , are idealized as point loads that are assumed to develop at the tips of the flange as the T-stub is loaded. These forces could more accurately be modeled as non-uniform pressure distributions acting on the flange exterior of the tension bolts. The point load idealization, though, provides reasonable results with much less computational effort provided that the length of the flange exterior of the tension bolts is not large. To account for this in the model, the magnitude of the length a is limited to $1.25b$.

$$a' = a + \frac{d_b}{2} \quad (2)$$

$$b' = b - \frac{d_b}{2} \quad (3)$$

where

d_b = diameter of the bolt

The parameter α is defined as the ratio of the moment at the bolt line to the moment at the face of the T-stem, and is an indicator of the level of prying present. Physically, α is limited to values between 0 and 1. A value of 1 is achieved if the bolt is stiff enough to cause the flange to act as a fixed-fixed beam and a value of 0 results when the flange separates completely from the column. In calculating the prying capacity, however, α is not limited. If $\alpha \leq 0$ then the flange is in single curvature, the prying forces are zero, and the bolts are subjected to conventional tension only. If $\alpha \geq 1$ then the flange is in double curvature and the prying forces are maximized. When $0 \leq \alpha \leq 1$, a combination of flange yielding and bolt prying will occur (Thornton, 1985). M is the moment at the face of the stem and δ is the ratio of the net section of the flange at the bolt line to the gross section at the face of the stem, excluding the fillet, and can be written as

$$\delta = 1 - \frac{d_h}{p} \quad (4)$$

where

d_h = diameter of the bolt hole

Moment equilibrium of the T-flange between the face of the stem and the bolt line (Figure 4), using b' , results in Equation 5, moment equilibrium of the flange to the exte-

rior of the bolt line, using a' , results in Equation 6, and force equilibrium of the entire flange results in Equation 7.

$$T \times b' = [1 + (\sigma \times \delta)] M \quad (5)$$

$$Q \times a' = \alpha \times \delta \times M \quad (6)$$

$$B = T + Q \quad (7)$$

Equation 5 can be solved for α as is shown in Equation 8.

$$\alpha = \left(\frac{1}{\delta} \right) \left(\frac{T \times b'}{M} - 1 \right) \quad (8)$$

At failure, M will be the plastic moment capacity of the flange and can be written as

$$M_p = \left(\frac{p \times t_f^2}{4} \right) F_y \quad (9)$$

Substitution of M_p into Equation 8 yields α as a function of the applied load, T , as shown in Equation 10.

$$\alpha = \left(\frac{1}{\delta} \right) \left(\frac{4T \times b'}{p \times t_f^2 \times F_y} - 1 \right) \quad (10)$$

Manipulation of the equilibrium equations provides the prying force, Q , as

$$Q = T \left(\frac{\alpha \times \delta}{1 + (\alpha \times \delta)} \right) \left(\frac{b'}{a'} \right) \quad (11)$$

The capacity of an existing T-stub is calculated based on the minimum of Equations 12, 13, and 14 which correspond to a flange mechanism, mixed mode failure, and a tension fracture, respectively. These three equations represent the possible failure modes of the flange and tension bolts. As previously mentioned, a flange mechanism will develop if

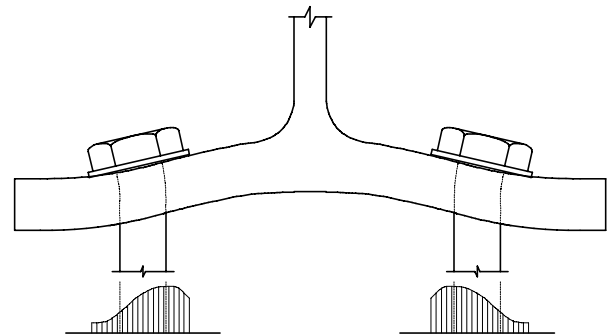


Fig. 5. Bolt head pressure distribution.

$\alpha \geq 1$, bolt prying combined with flange yielding will govern if $0 \leq \alpha \leq 1$, and conventional bolt strength with no prying governs if $\alpha \leq 0$. Note, however, that the capacity of an existing T-stub can be computed without calculating α . This is convenient because α is a function of the applied load per bolt, T , and the solution would otherwise be iterative.

$$T = \frac{(1+\delta)}{4b'} (p \times F_y \times t_f^2) \quad (12)$$

$$T = \frac{B_n \times a'}{a' + b'} + \frac{p \times F_y \times t_f^2}{4(a' + b')} \quad (13)$$

$$T = B_n \quad (14)$$

A solution space for a typical T-stub (TA-01) is shown in Figure 6. The solution space is the result of plotting a T-stub's flange capacity as a function of the flange thickness. The bold line OABC defines the capacity of the flange and tension bolts and the region below this line, OABCD, represents an adequate design. Segment OA defines the flange mechanism strength and is calculated using Equation 12 which assumes that $\alpha = 1$, segment AB is defined by the bolt capacity including the effects of prying and is computed using Equation 13, and segment BC represents the conventional strength of the bolts without prying and is computed as shown in Equation 14.

The line segment OB represents the case of $\alpha = 0$. The region OBCD represents a T-stub design with negligible prying effects, as would be desired when considering fatigue. The flange thickness associated with the point B is often referred to as the critical thickness, t_c , because a T-stub with a flange thickness greater than t_c will have negligible prying and will develop the full tensile strength of the

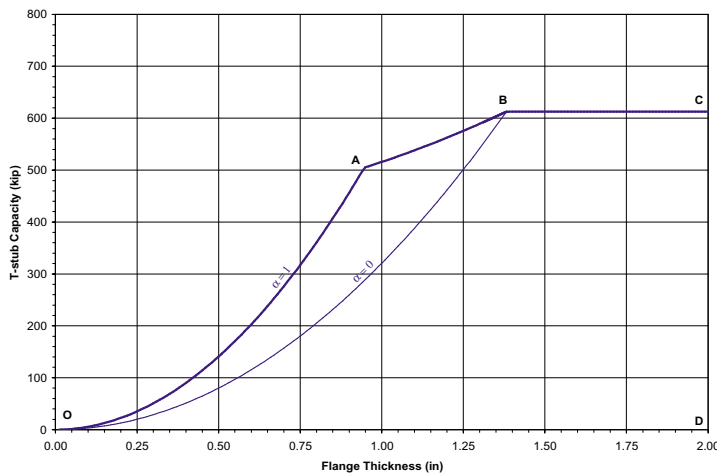


Fig. 6. Solution space for a typical T-stub for flange yielding and bolt prying.

bolts. The point A is generally considered to represent a balanced failure because the full strength of the flange is exhausted at the same time that the bolt forces, including prying, become critical (Astaneh, 1985). The critical thickness and balanced load are written as

$$t_c = \sqrt{\frac{4B_n \times b'}{p \times F_y}} \quad (15)$$

$$T_o = \frac{B_n}{1 + \left(\frac{\delta}{1+\delta} \right) \left(\frac{b'}{a'} \right)} \quad (16)$$

Figure 7 shows an expanded solution space. Line segment EFA represents a bolt failure after a flange mechanism has developed. The flange mechanism OA is a theoretical failure mode but does not represent the ultimate flange strength. After developing the mechanism, the flange is able to resist additional forces because of strain hardening of the material and because of membrane effects. Line OF represents a flange mechanism failure with a value of $\alpha = 2$. Although this case is outside the physical range of 0 to 1, it is interesting to note that the failure loads for many of the T-stubs tested in this investigation lie along line segment FA. Since the flanges of the T-stubs have exceeded their flange mechanism capacity ($\alpha = 1$) by the time they reach line segment FA, this portion of the curve represents a range of ductile flange behavior. A more rational means of defining this range will be presented later.

Figure 8 shows the capacity of a representative T-stub plotted as a function of the flange thickness and tension bolt gage. The figure is useful for illustrating the interaction between the primary parameters in flange behavior. The surface represents failure of the T-stub with all points below considered adequate. The two ridges shown as A1-A2-A3

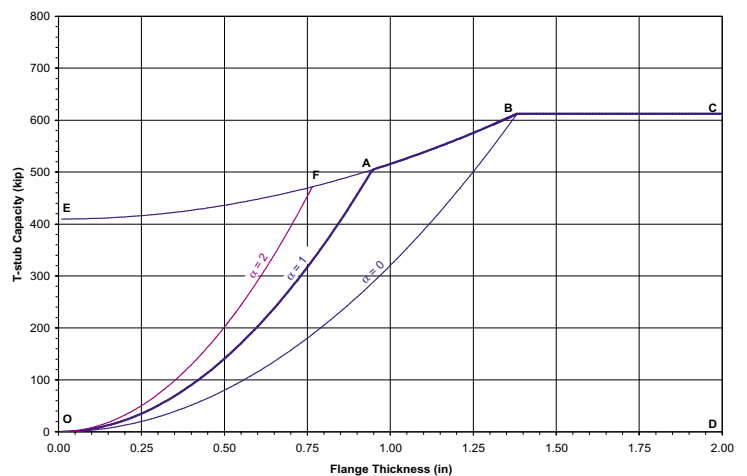


Fig. 7. Expanded solution space for flange yielding and bolt prying of a T-stub.

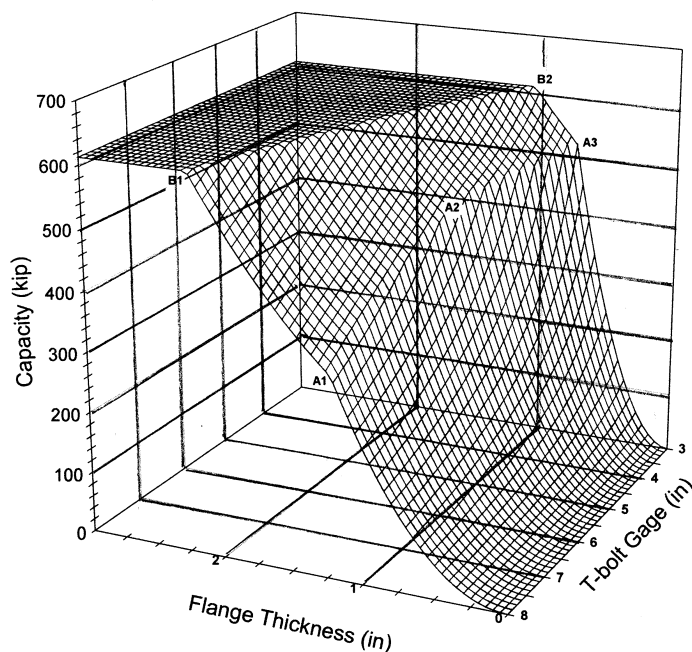


Fig. 8. Failure surface for flange yielding and bolt prying.

and B1-B2 correspond to points A and B in Figures 6 and 7 and represent changes in failure mode. The discontinuity at point A2 in Figure 8 is created by the limit that the length a must not exceed $1.25b$.

Figures 9, 10, and 11 show test results plotted on the solution curves for representative T-stubs tested during the SAC investigation. Figure 9 represents a T-stub with four $\frac{7}{8}$ -in. diameter A490 tension bolts, Figure 10 represents T-stubs with eight $\frac{7}{8}$ -in. diameter A490 tension bolts, and Figure 11 represents T-stubs with eight 1-in. diameter A490 tension bolts. The tension bolt failures, shown as solid symbols, should lie on or just above the capacity curves. The failures represent a broad range of conditions from pure tension as in the case of TA-17, combined prying and flange yielding as in the cases of TC-02 and TC-03, to the development of flange mechanisms as demonstrated by TC-11 and TC-12. The open symbols in Figure 11 represent a net section fracture of the stem of the T-stub. These failures should lie below the capacity curves. Note that although T-stubs TC-11 and TC-12 developed theoretical flange mechanisms, they were still able to achieve capacities predicted by the expanded prying curve (line segment FA in Figure 7).

While the solution space is useful for characterizing and comparing the behavior of the T-stubs, it does not provide a convenient means of evaluating the overall precision of the model. Table 1 contains the flange prying capacities for the

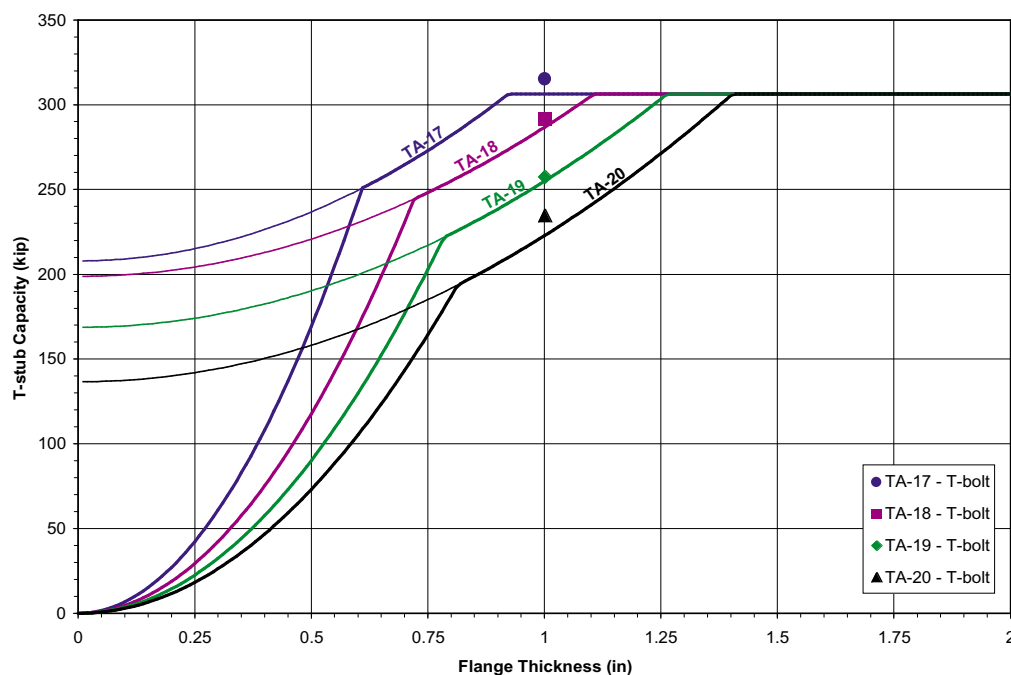


Fig. 9. Flange yielding/prying solution space for the representative T-stubs (four $\frac{7}{8}$ -in. dia. A490 tension bolts).

Table 1. Flange Mechanism/Prying Capacities by Model

Test ID	Exp. Capacity	T-Bolt Capacity	% Prying	Struik Capacity	% Error	Eurocode 3 Capacity	% Error	Douty & McGuire Capacity	% Error	Nair et al. Capacity	% Error	Modified Struik Capacity	% Error	Kato & McGuire Capacity	% Error
TA-03	451.09	612.51	35.8%	400.5	-11.2%	387.3	-14.1%	502.0	11.3%	331.8	-26.4%	429.2	-4.9%	433.1	-4.0%
TA-07	433.97	612.51	41.1%	400.5	-7.7%	387.3	-10.8%	502.0	15.7%	331.8	-23.5%	429.2	-1.1%	433.1	-0.2%
TA-04	388.88	612.51	57.5%	338.0	-13.1%	317.4	-18.4%	467.6	20.2%	283.5	-27.1%	362.3	-6.8%	370.7	-4.7%
TA-17	315.44	306.25	-2.9%	297.1	-5.8%	304.3	-3.5%	303.4	-3.8%	285.9	-9.4%	306.3	-2.9%	306.3	-2.9%
TA-18	291.70	306.25	5.0%	267.8	-8.2%	269.3	-7.7%	290.5	-0.4%	251.1	-13.9%	285.6	-2.1%	300.4	3.0%
TA-19	257.38	306.25	19.0%	236.6	-8.1%	234.4	-8.9%	277.9	8.0%	223.8	-13.0%	253.6	-1.5%	269.2	4.6%
TA-20	234.66	306.25	30.5%	205.4	-12.5%	199.4	-15.0%	268.5	14.4%	197.8	-15.7%	220.1	-6.2%	238.0	1.4%
TB-02	464.78	612.51	31.8%	424.7	-8.6%	417.6	-10.2%	529.8	14.0%	345.2	-25.7%	467.7	0.6%	459.3	-1.2%
TB-04	405.69	520.10	28.2%	374.4	-7.7%	370.8	-8.6%	449.8	10.9%	317.0	-21.9%	412.4	1.6%	409.0	0.8%
TB-09	315.07	306.25	-2.8%	297.2	-5.7%	306.3	-2.8%	306.7	-2.6%	269.7	-14.4%	306.3	-2.8%	306.3	-2.8%
TB-10	277.13	306.25	10.5%	258.1	-6.9%	262.4	-5.3%	295.6	6.7%	233.3	-15.8%	284.3	2.6%	292.7	5.6%
TC-01	584.72	606.67	3.8%	532.9	-8.9%	555.6	-5.0%	583.6	-0.2%	464.1	-20.6%	576.3	-1.4%	581.2	-0.6%
TC-02	525.38	606.67	15.5%	484.4	-7.8%	492.2	-6.3%	558.9	6.4%	414.7	-21.1%	522.1	-0.6%	527.7	0.4%
TC-03	468.16	606.67	29.6%	428.3	-8.5%	428.8	-8.4%	535.9	14.5%	367.6	-21.5%	461.6	-1.4%	471.6	0.7%
TC-04	416.97	606.67	45.5%	372.2	-10.7%	365.3	-12.4%	519.5	24.6%	318.4	-23.7%	401.2	-3.8%	415.5	-0.4%
TC-05	543.41	524.53	-3.5%	479.9	-11.7%	499.8	-8.0%	504.6	-7.2%	438.4	-19.3%	521.6	-4.0%	524.5	-3.5%
TC-07	446.34	524.53	17.5%	387.4	-13.2%	390.1	-12.6%	463.3	3.8%	345.9	-22.5%	417.6	-6.4%	430.8	-3.5%
TC-11	580.72	776.56	33.7%	521.7	-10.2%	508.7	-12.4%	656.4	13.0%	421.5	-27.4%	562.3	-3.2%	565.0	-2.7%
TC-12	512.56	776.56	51.5%	449.9	-12.2%	427.5	-16.6%	628.4	22.6%	358.6	-30.0%	484.9	-5.4%	493.2	-3.8%
TC-13	633.19	655.17	3.5%	572.7	-9.6%	588.6	-7.0%	614.3	-3.0%	491.8	-22.3%	618.9	-2.3%	621.0	-1.9%
TC-15	516.38	655.17	26.9%	460.0	-10.9%	451.6	-12.5%	553.8	7.3%	384.5	-25.5%	495.8	-4.0%	503.3	-2.5%
Average:				-9.5%		-9.8%		8.4%		-21.0%		-2.7%		-0.9%	
St. Deviation:				2.3%		4.2%		9.0%		5.5%		2.6%		2.8%	

All capacities are in kips

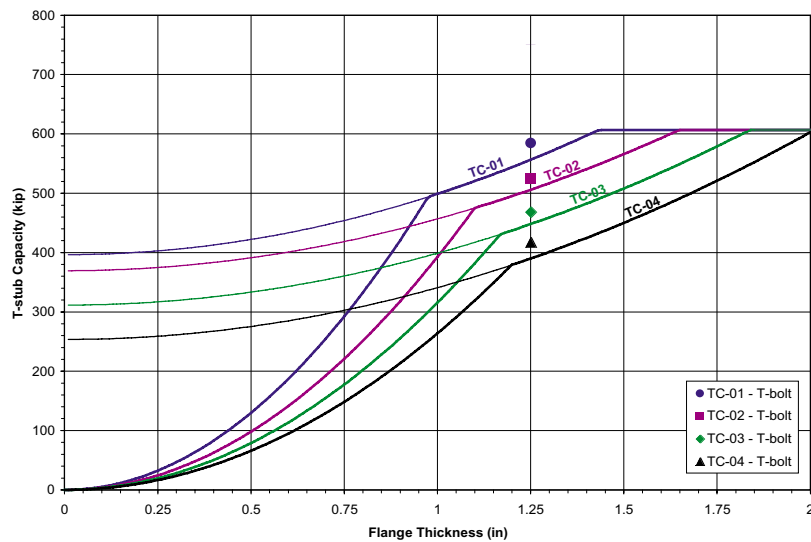


Fig. 10. Flange yielding/prying solution space for representative T-stub (eight $\frac{7}{8}$ -in. dia. A490 tension bolts).

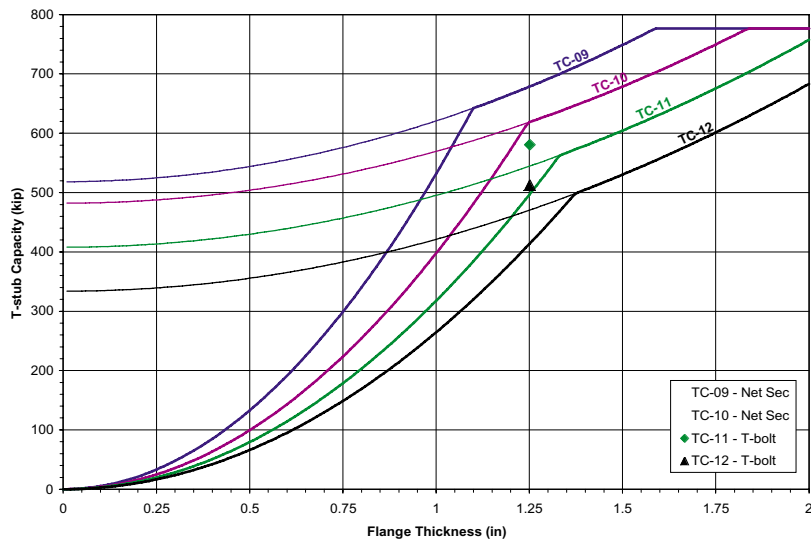


Fig. 11. Flange yielding/prying solution space for the T-stubs (eight 1-in. dia. A490 tension bolts).

21 T-stubs from the SAC investigation that failed with tension bolt failures. The column labeled “T-bolt Capacity” contains the capacity of the bolts without the effects of prying ($B_n \times n_{tb}$), the column labeled “Experimental Capacity” contains the maximum loads recorded during the testing of each T-stub, and the percent prying was calculated as

$$\% \text{ Prying} = \frac{(B_n \times n_{tb}) - \text{Experimental Capacity}}{\text{Experimental Capacity}} \quad (17)$$

The percent difference was calculated as

$$\% \text{ Difference} = \frac{\text{Predicted Capacity} - \text{Experimental Capacity}}{\text{Experimental Capacity}} \quad (18)$$

As a result, a negative percent difference represents a conservative capacity prediction. All predictions listed in Table 1 were computed using the actual material properties and are based on either the combined flange mechanism and bolt capacity ($0 \leq \alpha \leq 1$) determined by Equation 13 or the conventional bolt strength without prying ($\alpha \leq 0$) determined by Equation 14. No attempt was made to identify the load at which a flange mechanism formed ($\alpha \geq 1$). No resistance factors were used in the calculations.

The capacities predicted by the Struik model were all lower than the observed experimental capacities. The average percent difference was -9.5 percent with a standard deviation of 2.3 percent. The low standard deviation is an indication that the model is accurate. The under prediction of strength is likely related to location of the plastic hinge near the T-stem. The model assumes that a plastic hinge forms at the face of the stem. Yield lines on the test specimen, however, indicated that the hinge was located in the *k*-zone, a small distance away from the stem face. By moving the hinge away from the stem face, the moment arm, b' is reduced which lowers the moment in the flange at the stem and the prying force. Finally, the increased thickness of the flange in the *k*-zone and strain hardening of the material also increase the strength.

EUROCODE 3 MODEL

Annex J of the Eurocode 3 (Eurocode, 1993) addresses the design of beam-to-column connections. The model used by the Eurocode for flange strength closely resembles the theory developed by Struik and de Back. The code recognizes the same three failure modes documented by Struik. These limit states are shown as Equations 19, 20, and 21, which predict a flange mechanism, mixed mode failure, and simple tension bolt fracture, respectively.

$$T = \frac{p \times F_y \times t_f^2}{2m} \quad (19)$$

$$T = \frac{n \times B_n}{m+n} + \frac{p \times F_y \times t_f^2}{4(m+n)} \quad (20)$$

$$T = B_n \quad (21)$$

The primary differences between the Eurocode and the Struik model are the way that the flange dimensions are measured and the fact that the Eurocode makes no strength reduction for flange material lost to drilling of the bolt holes. The lengths m and n are illustrated in Figure 12. Like the dimension a in the Struik model, n is limited to a value no greater than $1.25m$. The length m is defined as the distance from the centerline of the bolt to the face of the stem, minus 80 percent of the radius of the fillet in the *k*-zone or 80 percent of the leg of a weld for welded T-stubs or end plates. The concentrated bolt forces are located at the center of the bolt line.

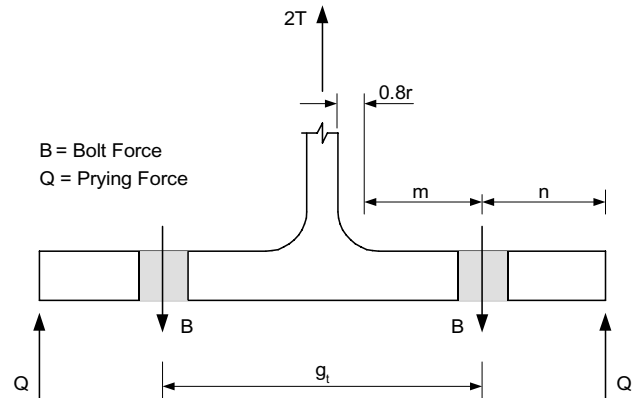


Fig. 12. Eurocode 3 T-stub dimensions.

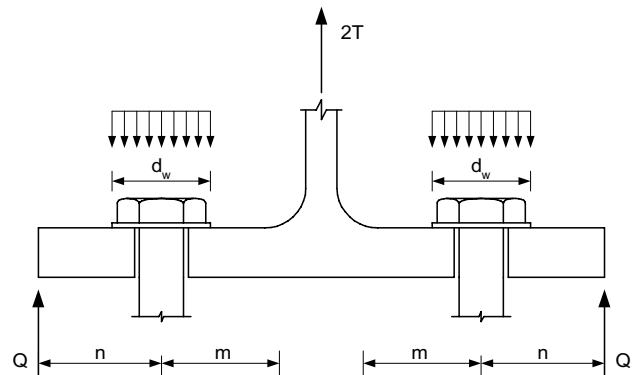


Fig. 13. Alternative eurocode force distribution (Jaspart model).

A comparison of the Eurocode equations to Struik's model shows that the capacity of the flange for a flange mechanism failure as predicted by the Eurocode is the same as that predicted by Struik's model assuming that δ is 1 and neglecting the differences between b and m . The prying capacity for a mixed mode failure in the Eurocode is identical to that predicted by Struik, again neglecting the differences between b and m . A provision for an alternative method for calculating the mechanism capacity of the flange based on work by Jaspart (1991) is also provided.

Flange capacities predicted using the Eurocode equations are shown in Table 1. The average percent difference of the predictions is -9.8 percent with a standard deviation of 4.2 percent. No resistance factors were used for the Eurocode capacity predictions.

JASPART MODEL

The method developed by Jaspart (1991) models the force applied to the flange by a bolt as a pressure uniformly distributed over the diameter of the washer as shown in Figure 13 and was derived considering the negative work done by a portion of the bolt pressure. This formulation leads to a higher prediction of the flange mechanism capacity. The capacity of the alternative model is calculated as shown in Equation 22 and a graphical comparison is made to the model of Struik and de Back in Figure 14. The curves plotted in Figure 14 were calculated for T-stub TA-01 and the values of a' and b' were substituted for n and m , respectively, in Equation 22.

$$T = \frac{\left(4n - \frac{d_w}{4}\right) \times p \times F_y \times t_f^2}{(8m \times n) - d_w(m+n)} \quad (22)$$

As was mentioned earlier, several experimental flange failures fell along the portion of solution space defined by line segment FA in Figure 7. These failures would be considered ductile because of the significant flange deformations and energy dissipation associated with a flange mechanism. The definition of the point F in Figure 7, however, is based on a value of $\alpha = 2$ that is not physically possible. A comparison of Figures 7 and 14, though, shows that the flange mechanism capacity as predicted by Jaspart could be used to define a ductile range of flange behavior. Since this approach is more rational than using a value of $\alpha = 2$, it is recommended.

DOUTY AND MCGUIRE MODEL

Douty and McGuire (Douty, 1964; Douty and McGuire, 1965) developed a prying model based on a simple beam model. The models were developed by considering the elastic stiffness of the flange under the compression of the bolt forces and the elastic stiffness of the bolts themselves. The model uses the dimensions a and b as previously defined but makes no adjustment for the assumption that the bolt forces will be concentrated along the inside of the bolts. No limit is placed on the value of a but the authors acknowledge the limitation of the point load assumption for the location of the prying forces. Two equations for the prying force, Q , were developed. Equation 23 represents a prediction for the system before the flange separates from the column and Equation 24 represents the flange after separation. The flange is assumed to remain elastic in both cases.

$$Q = T \left[\frac{\frac{1}{2} - \frac{E \times p \times t_f^3}{12 \times a \times b^2 (r_b + r_p)}}{\left(\frac{a}{b}\right) \left(\frac{a}{3b} + 1\right) + \frac{E \times p \times t_f^3}{12 \times a \times b^2 (r_b + r_p)}} \right] \quad (23)$$

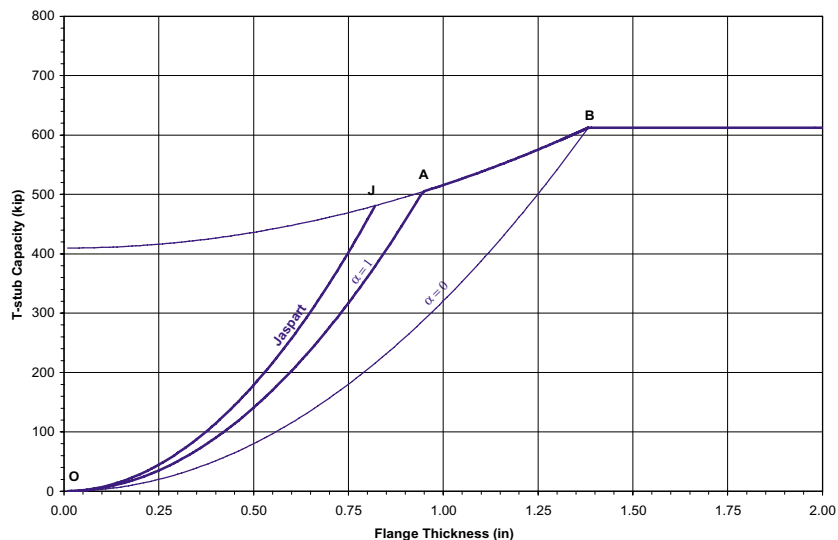


Fig. 14. Comparison of Jaspart's model with that of Struik and de Back.

$$Q = T \left[\frac{\frac{1}{2} - \left(\frac{E \times p \times t_f^3}{12 \times a \times b^2 (r_b + r_p)} \right) \left(1 - \frac{B_o}{T} \right)}{\left(\frac{a}{b} \right) \left(\frac{a}{3b} + 1 \right) + \frac{E \times p \times t_f^3}{12 \times a \times b^2 (r_b + r_p)}} \right] \quad (24)$$

Because of the complexity of these formulas, the semi-empirical formulation shown as Equation 25 was developed. It shows the prying force as a function of the flange thickness, bolt location, and bolt size. This semi-empirical model was also thought to be too complicated for design purposes and was further reduced to that shown in Equation 26. The capacities as calculated using Douty and McGuire's models are shown compared to that of Struik and de Back in Figure 15 for T-stub TA-01. Obviously, each of these two models would require an upper limit based on the tensile capacity of the connectors without prying.

$$Q = T \left[\frac{\frac{1}{2} - \frac{p \times t_f^4}{30 \times a \times b^2 \times A_b}}{\left(\frac{a}{b} \right) \left(\frac{a}{3b} + 1 \right) + \frac{p \times t_f^4}{6 \times a \times b^2 \times A_b}} \right] \quad (25)$$

$$Q = T \left(\frac{3 \times b}{8 \times a} - \frac{t_f^3}{20} \right) \quad (26)$$

The predicted values calculated using the semi empirical model are given in Table 1. The average percent difference was 8.4 percent with a standard deviation of 9.0 percent.

Most of the predicted capacities were higher than the experimental ones indicating an unconservative model. The larger deviation indicates that the model is not as accurate as that of Struik. An examination of the results shows a trend in the model accuracy that appears to be tied to the handling of the tension bolt gage, g_t . The model is less accurate for wider bolt gages.

Douty (1964) also recognized the possibility of a ductile flange fracture when the flange thickness is sufficiently thin. Although no failures of this nature were observed during the research investigation conducted at Georgia Tech, Douty reported an experiment in which the flange of a T-stub fractured after sustaining significant bending strains. Based on this failure, Douty developed an equation that predicts the load that will cause a ductile flange fracture near the k -line. A modified version of the equation is shown as Equation 27.

$$T = \left(\frac{E_s \times I}{b} \right) \left(\frac{2 \times \epsilon_{fract}}{t_f} - \frac{s \times M_p}{E_s \cdot I} \right) + \frac{M_p}{b} \quad (27)$$

where

- E_s = modulus of elasticity of steel
- I = the moment of inertia of the T-stub flange (entire width)
- ϵ_{fract} = fracture strain of the material
- M_p = plastic moment of the flange as shown in Equation 9
- s = the ratio of curvature on the onset of hardening to the curvature corresponding to the formation of a plastic hinge

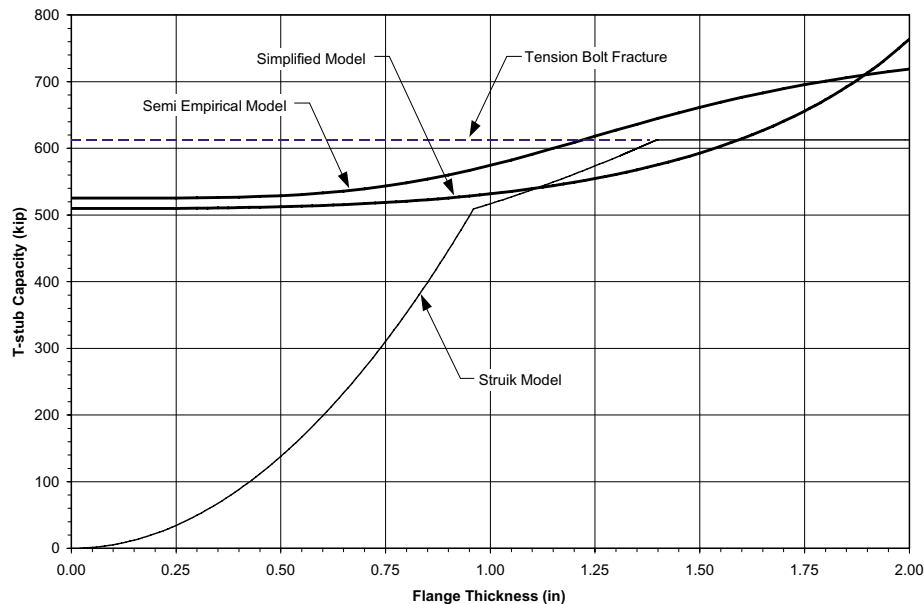


Fig. 15. Comparison of Douty and McGuire's prying models to that of Struik and de Back.

Table 2. Comparison of the Modified Struik Prying Model with Douty's Test Data

Test ID	Exp Capacity	T-bolt Capacity	% Prying	Modified Bolt	Struik & de Back % Diff
A1	176.00	224.00	27.3%	161.24	-8.4%
A3	236.00	248.00	5.1%	248.00	5.1%
A7	392.00	408.00	4.1%	408.00	4.1%
A9	177.00	224.00	26.6%	165.79	-6.3%
A11	256.00	247.00	-3.5%	247.20	-3.4%
A12	245.00	239.00	-2.4%	239.20	-2.4%
A15	404.00	400.00	-1.0%	400.00	-1.0%
B1	202.00	256.00	26.7%	180.60	-10.6%
B6	253.00	240.00	-5.1%	240.00	-5.1%
B7	233.00	222.00	-4.7%	222.00	-4.7%
B9	347.00	388.00	11.8%	388.00	11.8%
B10	403.00	396.00	-1.7%	396.00	-1.7%
B12	378.00	400.00	5.8%	400.00	5.8%
All capacities are in kips				Average:	-1.3%
				St Dev:	6.4%

NAIR ET AL. MODEL

Nair, Birkemoe, and Munse (1974) investigated T-stub connections at the University of Illinois and developed empirical capacity equations. The investigation made use of pairs of T-stubs tested back-to-back. The flanges of two T-stubs were bolted together with a spacer plate between them. The T-stubs were subjected to fatigue loading, monotonic loads, and cyclic loads. One disadvantage of using the back-to-back set up is that the tension bolts are subjected to a higher level of bending than would be experienced when bolted to a rigid plate or column flange. Two equations were developed. Equation 28 was calibrated for T-stubs using A325 bolts and Equation 29 was calibrated for T-stubs using A490 bolts.

$$Q = T \left(\frac{(100 \times b \times d_b^2) - (18 \times p \times t_f^2)}{(70 \times a \times d_b^2) + (21 \times p \times t_f^2)} \right) \quad (28)$$

$$Q = T \left(\frac{(100 \times b \times d_b^2) - (14 \times p \times t_f^2)}{(62 \times a \times d_b^2) + (21 \times p \times t_f^2)} \right) \quad (29)$$

The length a in Equations 28 and 29 is the same as that shown in Figure 4 and is limited to a value no greater than $2t_f$. The length b is the same as that used in the test shown in Figure 4 except that $1/16$ in. is subtracted, apparently to account for the fillet of the K-zone between the stem and flange. Because the equations are entirely empirical, they are only valid for T-stubs similar to those tested. The equations are based on tests of T-stubs fabricated from A36 steel with a flange thickness of $1\frac{1}{16}$ in. and a stem thickness of $1\frac{1}{16}$ in. The flange widths ranged from $6\frac{1}{2}$ in. to $9\frac{1}{2}$ in. and $\frac{3}{4}$ -in. diameter A325 and A490 bolts were used. Capacities

predicted using the model are shown in Table 1. The average percent difference was -21.0 percent with a standard deviation of 5.5 percent.

MODIFIED STRUIK MODEL

The prying and flange strength model recommended by Struik and de Back (Struik and de Back, 1969; Kulak et al., 1987) provided the highest level of accuracy of all the prying models evaluated. Better accuracy can be achieved, however, if the dimensions used in the calculations are modified slightly. If it is recognized that the fillet of the k -zone provides sufficient stiffness to shift the plastic hinge away from the face of the T-stem, the accuracy of the model is improved slightly. This can be accomplished by deducting a portion of the fillet radius from the dimension, b . A value of $0.80r$ is used in the Eurocode model. However, a value of $0.50r$ produces the highest degree of correlation between the model and experimental results and is recommended by the author. Since the k -zone fillet is not an actual circular fillet, however, the deduction should be presented more formally as

$$\frac{k_1}{2} - \frac{t_s}{4} \quad (30)$$

For implementation of this modification, it is convenient to introduce a new parameter, $t_{s,eff}$, the effective stem thickness, as

$$t_{s,eff} = k_1 + \frac{t_s}{2} \quad (31)$$

The effective stem thickness is illustrated in Figure 16. The length b is then calculated as

$$b = \frac{g_t - t_{s,eff}}{2} \quad (32)$$

and all subsequent calculations are performed as before.

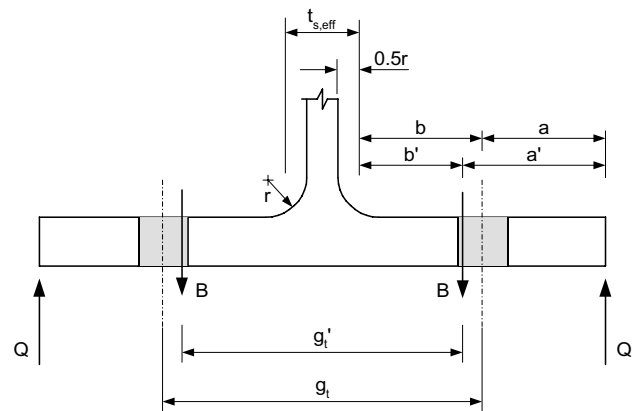


Fig. 16. Illustration of the effective stem thickness.

Incorporating the modification into the method reduces the average percent difference from -9.5 to -2.7 percent with a standard deviation of 2.5 percent for the 21 tests governed by prying failures. The model was also evaluated using test data obtained by Douty (1964). The results are shown in Table 2. The average percent difference with respect to Douty's test data is -1.3 percent with a standard deviation of 6.4 percent. This evaluation is important because the T-stubs tested by Douty were configured with four tension bolts while the majority of those tested in the SAC investigation at Georgia Tech were configured with eight tension bolts.

KATO AND MCGUIRE

While the most widely accepted strength models are based on the formation of a plastic flange mechanism, Douty (1964) observed that the force required to form a plastic flange mechanism does not necessarily represent the maximum force that a T-stub can resist. While recognizing that thinner flanges may be susceptible to ductile fracture at high bending strains, Douty noted that because of strain hardening in the plastic hinges, a flange which has formed a plastic mechanism based on the yield stress of the material can sustain additional load which may lead to a prying fracture of the tension bolts. The author agrees with this observation.

Based on observed post-elastic strength observed during the tests documented by Douty (1964), Kato and McGuire (1973) suggested using the ultimate strength of the T-stub material instead of the yield strength for predicting the ultimate strength of T-stub connections. This idea was explored further by Thornton (1992) by using Struik and de Back's model with F_u instead of F_y . The results were found to correlate quite well to experimental data reported by Douty and McGuire (1965). The predicted capacities for the T-stub specimens tested at Georgia Tech resulting from this approach are reported in Table 1 under the column labeled "Kato & McGuire." An average percent difference of -0.9 percent with a standard deviation of 2.8 percent was found.

CONCLUSIONS AND DISCUSSION

Several prominent prying models were discussed and evaluated using experimental data collected during a SAC investigation at the Georgia Institute of Technology as a basis. Prying models developed by Struik and de Back (1969), Nair et al. (1974), Douty and McGuire (1965), Kato and McGuire (1973), and Jaspart (1991) were considered in addition to the model that appears in the European design specification. The model developed by Struik and de Back, when used with the ultimate strength of the T-stub material,

provided the least difference between the predicted capacities and experimental data.

No attempt was made to identify the point during an experiment at which a plastic mechanism had formed in the flange of a T-stub. As a result, the model comparisons presented in Table 1 are based on either the mixed-mode (Equation 13) or pure tension strength (i.e. no prying - Equation 14).

ACKNOWLEDGMENTS

The research work leading to the findings presented in this paper was conducted under the direction of Dr. Roberto T. Leon at the Georgia Institute of Technology and was funded by SAC as subtask 7.03 and the Mid-America Earthquake Center under task ST7. SAC is a joint venture made up of the Structural Engineers Association of California (SEAOC), the Applied Technology Council (ATC), and the California Universities for Research in Earthquake Engineering (CUREE). SAC is funded by the Federal Emergency Management Association (FEMA).

REFERENCES

- AISC (1993), *Load and Resistance Factor Design of Structural Steel Buildings*, American Institute of Steel Construction, Chicago, IL, December 1.
- Astaneh, A., (1985), "Procedure for Design and Analysis of Hanger-type Connections," *Engineering Journal*, American Institute of Steel Construction, Vol. 22, No. 2.
- CISC (1997), *Handbook of Steel Construction*, 7th ed., Canadian Institute of Steel Construction, Willowdale, Ontario.
- Douty, R. T. (1964), *Strength Characteristics of High Strength Bolted Connections with Particular Application to the Plastic Design of Steel Structures*, Ph.D. Dissertation, Cornell University.
- Douty, R. T. and McGuire, W. (1965), "High Strength Bolted Moment Connections," *Journal of the Structural Division*, April, Vol. ST2, American Society of Civil Engineers.
- Eurocode (1993), *Design Procedures to C-EC3 - Concise Eurocode 3 for the Design of Steel Buildings in the United Kingdom*, The Steel Construction Institute.
- Fisher, J. W. and Struik, J. H. A. (1974), *Guide to Design Criteria for Bolted and Riveted Joints*, John Wiley & Sons, New York.
- Jaspart, J. P., and Maquoi, R. (1991), "Plastic Capacity of End-Plate and Flange Cleated Connections - Predictions and Design Rules," *Proceedings of the 2nd International Workshop on Connections in Steel Structures: Behavior, Strength and Design*, Pittsburgh, PA, April.

- Kato, B. and McGuire, W. (1973), "Analysis of T-stub Flange-to-Column Connections," *Journal of the Structural Division*, American Society of Civil Engineers, May, Vol. ST5.
- Kulak, G. L., Fisher, J. W., and Struik, J. H. A. (1987), *Guide to Design Criteria for Bolted and Riveted Joints*, 2nd ed., John Wiley & Sons, New York.
- Nair, R. S., Birkemoe, P. C., and Munse, W. H. (1974), "High Strength Bolts Subject to Tension and Prying," *Journal of the Structural Division*, American Society of Civil Engineers, February, Vol. ST2.
- Struik, J. H. A., and de Back, J. (1969), "Tests on Bolted T-stubs with Respect to Bolted Beam-to-Column Connections," Report 6-69-13, Stevin Laboratory, Delft University of Technology, Delft, The Netherlands.
- Swanson, J. A., and Leon, R. T. (2000), "Bolted Steel Connections: Tests on T-stub Components," *Journal of Structural Engineering*, American Society of Civil Engineers, January, 2000.
- Swanson, J. A. and Leon, R. T. (2001), "Stiffness Modeling of Bolted T-stub Connection Components," *Journal of Structural Engineering*, American Society of Civil Engineers, May 2001 (in-press).
- Swanson, J. A., Kokan, D. S., and Leon, R. T. (2001), "Advanced Finite Element Modeling of Bolted T-stub Connection Components," *Journal of Constructional Steel Research*, (in-press).
- Thornton, W. A., (1985), "Prying Action—A General Treatment," *Engineering Journal*, American Institute of Steel Construction, Vol. 22, No. 2.

NOTATION

a	Distance measured from the bolt line to the edge of the T-stub flange
a'	Distance measured from the bolt line to the edge of the T-stub flange plus half the bolt diameter
b	Distance from the bolt line to the face of the T-stem
b'	Distance from the bolt line to the face of the T-stem less half the bolt diameter
b_f	Flange width of a section

d_b	Diameter of a bolt
d_h	Diameter of a bolt hole
d_w	Diameter of a washer (assumed to be twice the diameter of a bolt)
g_i	Distance between the center lines of the tension bolts
k_f	Fillet dimension between the flange and web of a rolled section
m	Distance measured from the bolt line to the edge of the T-stub flange
n	Distance from the bolt line to the face of the T-stem less 80% of the fillet radius
n_{tb}	Number of tension bolts connecting the T-stub flange
p	Width of a T-stub that is tributary to one pair of bolts
s	Ratio of curvature on the onset of hardening to the curvature corresponding to the formation of a plastic hinge
t_c	Critical flange thickness above which prying forces are negligible
t_f	Thickness of a T-stub flange
$t_{s,eff}$	Effective stem width of a T-stub
A_b	Area of a bolt
B	Force present in a tension bolt at any given time
B_n	Tensile capacity of a bolt
B_o	Initial pretension of a bolt
E_s	Modulus of elasticity of steel
F_y	Yield stress of steel
I	Moment of inertia of a T-stub flange
M	Moment in a T-stub flange
M_p	Plastic moment of a T-stub flange
Q	Prying force per bolt
T	Applied T-stub tension per tension bolt
T_o	Applied load T-stub tension per bolt representing a balanced failure
W_{T-stub}	Width of the T-stub at the column flange
α	Ratio of the moment at the bolt line to the moment at the face of the T-stem
δ	Ratio of the net section of the flange at the bolt line to the gross section at the face of the stem, excluding the fillet
ϵ_{fract}	Strain at fracture for steel